doi:10.1038/nature06864

ARTICLES

Lateral presynaptic inhibition mediates gain control in an olfactory circuit

Shawn R. Olsen[1] & Rachel I. Wilson[1]

Olfactory signals are transduced by a large family of odorant receptor proteins, each of which corresponds to a unique glomerulus in the first olfactory relay of the brain. Crosstalk between glomeruli has been proposed to be important in olfactory processing, but it is not clear how these interactions shape the odour responses of second-order neurons. In the *Drosophila* antennal lobe (a region analogous to the vertebrate olfactory bulb), we selectively removed most interglomerular input to genetically identified second-order olfactory neurons. Here we show that this broadens the odour tuning of these neurons, implying that interglomerular inhibition dominates over interglomerular excitation. The strength of this inhibitory signal scales with total feedforward input to the entire antennal lobe, and has similar tuning in different glomeruli. A substantial portion of this interglomerular inhibition acts at a presynaptic locus, and our results imply that this is mediated by both ionotropic and metabotropic receptors on the same nerve terminal.

A sensory stimulus generally triggers activity in multiple neural processing channels, each of which carries information about some feature of that stimulus. The concept of a processing channel has a particularly clear anatomical basis in the first relay of the olfactory system, which is typically divided into glomerular compartments. Each glomerulus receives input from many first-order olfactory receptor neurons (ORNs), all of which express the same odorant receptor. Each second-order neuron receives direct ORN input from a single glomerulus, and thus all the first- and second-order neurons corresponding to a glomerulus constitute a discrete processing channel. An odorant typically triggers activity in multiple glomeruli, and local interneurons that interconnect glomeruli provide a substrate for crosstalk between channels.

The *Drosophila* antennal lobe is a favoured model for investigating olfactory processing because it contains only ~50 glomeruli[1], each of which corresponds to an identified type of ORN and an identified type of postsynaptic projection neuron (PN)[2–5]. Several recent studies of the *Drosophila* antennal lobe have produced divergent views regarding the relative importance of interglomerular connections. One model proposes that PN odour responses are almost completely determined by feedforward excitation[6,7]. This model ascribes little importance to crosstalk between glomerular processing channels. An alternative model proposes that interglomerular connections make an important contribution to shaping PN odour responses[8–12]. However, this has not been demonstrated by showing a change in PN odour responses when lateral inputs to that PN are removed. (We use the word 'lateral' as a synonym for 'interglomerular'.)

In principle, several features of olfactory processing in the *Drosophila* antennal lobe could reflect either intra- or interglomerular events. For example, most PNs are more broadly tuned to odours than their presynaptic ORNs[8,10]. This could reflect a purely intraglomerular nonlinear process, such as short-term synaptic depression at ORN–PN connections. Alternatively, it could be due to the fact that lateral excitatory connections exist between glomeruli[7,11,12]. It is also unclear whether inhibitory epochs in PN odour responses[8–10] reflect inter- or intraglomerular events. Many interneurons that are immuno-positive for GABA (γ-aminobutyric acid) form connections between glomeruli[9,13,14], but several recent studies have failed to observe any interglomerular inhibition[7,11,12]. These studies removed all the direct ORN inputs to an identified PN, and asked whether lateral input could be evoked in that PN by olfactory stimulation of other ORN types. In all cases, lateral inputs to PNs were excitatory. This raises the possibility that interglomerular inhibition might not exist, and that inhibitory PN odour responses might merely reflect intraglomerular feedback[15–17]. This is an important issue because intra- and interglomerular inhibition have different consequences for how olfactory representations are transformed in this circuit.

In this study, we address three questions. Do interglomerular interactions make a substantial contribution to PN odour responses? Do these interactions include lateral inhibition? If so, how does this occur, and why has it been difficult to observe?

Removing lateral input to projection neurons

We began by investigating what happens to PN odour responses when most lateral input to that PN is removed. We took advantage of the fact that the fly has two olfactory organs. About 90% of ORNs are contained in the antennae, whereas 10% are in the maxillary palp (Fig. 1a). Palp ORNs express odorant receptors not expressed in the antennae, and project to palp glomeruli that are distinct from glomeruli targeted by antennal ORNs[3,4]. Antennal and palp glomeruli are interconnected by local interneurons. Acute removal of the antennae eliminates 90% of the input to the antennal lobe, and therefore most excitatory drive to local interneurons (Fig. 1b). If lateral connections are mainly excitatory[7,11,12], then removing the antennae should decrease the odour responses of palp PNs.

We performed this experiment in two different palp glomeruli (VM7 and VC1). Surprisingly, removing the antennae increased most of the odour responses of these PNs (Fig. 1c, d and Supplementary Figs 2 and 3). No odour responses were decreased. This implies that most of our odours normally evoke lateral inhibitory input to these glomeruli, and that this outweighs the effect of lateral excitatory input.

We examined the input–output function of each glomerulus by plotting the strength of each PN odour response against the strength of the cognate ORN response to the same odour. These input–output functions were nonlinear (Fig. 1d), which is typical for most glomeruli[10]. When we removed most lateral input to VM7 and VC1 PNs,

[1]Department of Neurobiology, Harvard Medical School, 220 Longwood Avenue, Boston, Massachusetts 02115, USA.

the nonlinearity persisted (Fig. 1d) and these PNs became even more broadly tuned (Fig. 1e). This argues that broad tuning of PNs[8,10] results mainly from purely intraglomerular mechanisms. These could include short-term synaptic depression at ORN–PN connections and/or an intrinsic ceiling on PN firing rates. Lateral excitation should tend to broaden PN tuning even more, but lateral inhibition evidently counteracts this.

One clue to the significance of lateral inputs is that, in the intact antennal lobe circuit, PN responses cannot be predicted purely on the basis of feedforward excitatory inputs[10]. Two odours can elicit similar responses in an ORN but divergent responses in a postsynaptic PN. For example, pentyl acetate and 4-methyl phenol evoke similar activity in VM7 ORNs but not in VM7 PNs (Fig. 1c), implying that these odours recruit different lateral inputs to this glomerulus. After antennae were removed, these odours evoked similar responses in VM7 PNs (Fig. 1c). Overall, removing the antenna increased the correlation between the ranked odour preferences of ORNs and their cognate PNs (Spearman's ρ increased from 0.82 to 0.88 for VM7 and from 0.89 to 0.94 for VC1; $P < 0.02$ for each comparison, Mann–Whitney U-test).

Lateral inhibition suppresses ORN input

Several recent studies have failed to observe lateral inhibition in the *Drosophila* antennal lobe[7,11,12]. These studies silenced all direct ORN inputs to a PN and focused on lateral input to that PN evoked by stimulating ORNs presynaptic to other glomeruli. We reasoned that some lateral inhibition might target ORN axon terminals; if so, this would only be observed when the direct ORN inputs to a PN are active. GABAergic inhibition at ORN axon terminals in the olfactory bulb has been described previously[15–21], and synapses from GABAergic interneurons onto ORN axon terminals have been found in an insect antennal lobe[22].

To test the idea that some lateral inhibition is presynaptic, we asked how lateral input to glomerulus VM7 depends on the activity of VM7 ORNs. Each VM7 ORN fires spontaneously at ~10 spikes s^{-1}, and consequently these PNs are bombarded by spontaneous spike-driven excitatory postsynaptic potentials (EPSPs; Supplementary Fig. 4a). When we silenced VM7 ORNs by removing the maxillary palps, large spontaneous EPSPs disappeared in VM7 PNs (Fig. 2a). In this experimental configuration, stimulating the antennae with odorants depolarized VM7 PNs (Fig. 2a), which is consistent with previous reports that lateral input is excitatory when direct ORN inputs are silent[7,11,12]. Next, we asked whether preserving spontaneous activity in VM7 ORNs would allow us to observe lateral inhibition. To prevent odour-evoked activity in VM7 ORNs, we covered the maxillary palps

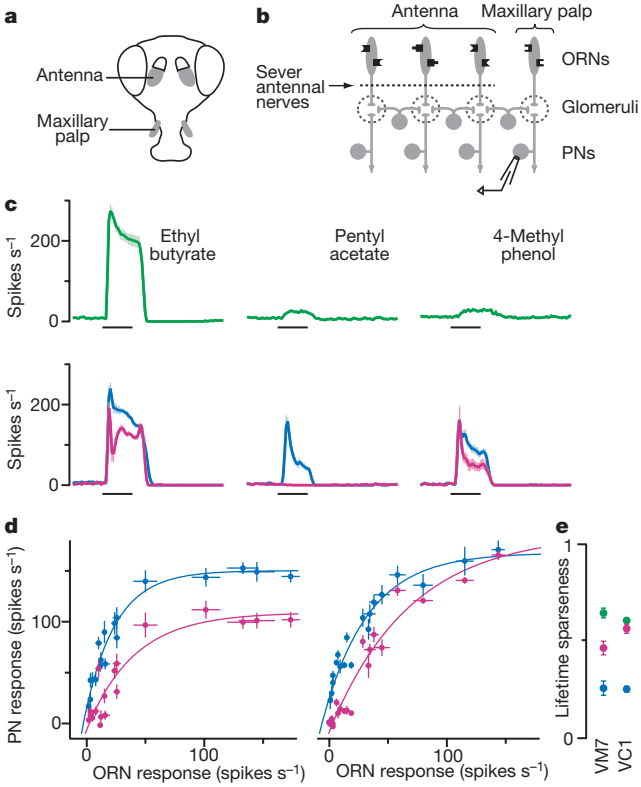

Figure 1 | Removing lateral input disinhibits projection neurons. **a**, *Drosophila* olfactory organs. **b**, Experimental configuration. **c**, Spiking responses of ORNs (green) and PNs (blue and magenta) for the palp glomerulus VM7 ($n = 4$–12 for each response). PNs are shown with (magenta) and without (blue) lateral input from antennal glomeruli. The black bars represent the 500-msec odour-stimulus period. **d**, Input–output functions for palp glomeruli VM7 (left) and VC1 (right). Each point represents the average PN response to an odour versus the response of the cognate ORNs. PNs are shown with antennae intact (magenta) or removed (blue). Responses to 18 out of 20 odours are significantly disinhibited in VM7; 13 out of 20 are significantly disinhibited in VC1 ($P < 0.05$, t-tests). **e**, Odour selectivity of ORNs (green) and cognate PNs with antennae intact (magenta) or removed (blue). Lifetime sparseness is 0 for an unselective cell and 1 for a maximally selective cell. All within-glomerulus comparisons are significant ($P < 0.002$, Mann–Whitney U-test), except ORNs versus antennae-intact PNs for VC1. Data are shown as mean ± s.e.m.

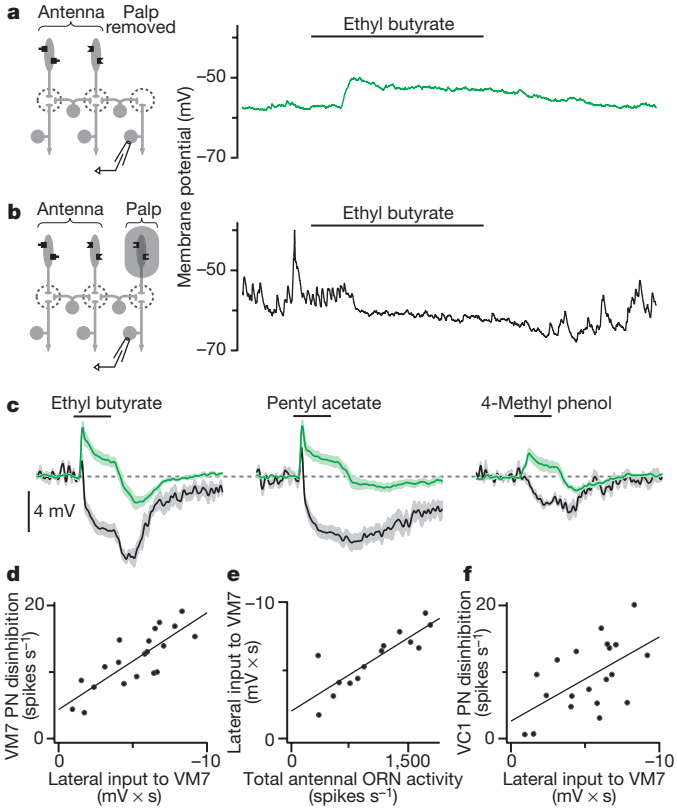

Figure 2 | Lateral inhibition suppresses spontaneous EPSCs and scales with total ORN input. **a**, Left: experimental configuration. Right: recording from a PN in glomerulus VM7. Olfactory stimulation evokes depolarization. Spontaneous EPSPs are absent. **b**, Left: palps are shielded from odours. Right: recording from a PN in glomerulus VM7. Olfactory stimulation suppresses spontaneous EPSPs. **c**, Average VM7 PN responses as in **a** (green) or **b** (black); $n = 6$–7 PNs for each condition. When ORNs are shielded (black), inhibition dominates. When ORNs are absent (green), excitation dominates throughout the stimulus period. (Off-inhibition probably reflects lateral postsynaptic inhibition, see Supplementary Fig. 5.) Pale bands are s.e.m. **d**, Lateral input to VM7 (as in **b**) is correlated with the disinhibition in VM7 PNs after antennal removal (see Fig. 1b). Each point represents a different odour. Lateral input is measured as the time-integrated change in membrane potential. **e**, Lateral input to VM7 is correlated with total antennal ORN spiking activity evoked by each odour. **f**, Lateral input to VM7 is correlated with the disinhibition in VC1 PNs after antennal removal.

with a plastic shield. We inferred that the shield did not prevent spontaneous activity in VM7 ORNs because we observed normal spontaneous EPSPs in VM7 PNs (Fig. 2b). The shield was clearly an effective barrier to odours because it blocked the normal strong excitatory response to ethyl butyrate in VM7 PNs (Supplementary Fig. 4). Instead, when the palps were shielded, stimulating the antennae with odorants suppressed spontaneous EPSPs in VM7 PNs (Fig. 2b, c). This was accompanied by hyperpolarization of the membrane potential, which would reflect (at least in part) the removal of ongoing depolarization produced by EPSP bombardment.

For all 20 odours in our panel, lateral input depolarized VM7 PNs when their cognate ORNs were absent (as in Fig. 2a) and hyperpolarized these PNs when their ORNs were spontaneously active (as in Fig. 2b). This argues that a substantial component of lateral inhibition acts at a presynaptic locus. This does not mean that all lateral inhibition is presynaptic; indeed there is evidence for an additional postsynaptic component (Supplementary Fig. 5).

Inhibition scales with total ORN input

When palp ORNs were shielded, different odours evoked different amounts of inhibition in glomerulus VM7 (Fig. 2c, black traces). We hypothesized that this odour tuning could explain why antennal removal disinhibits some VM7 PN odour responses more than others (Fig. 1c, d). To test this, we measured the amount of inhibition evoked by each odour in the shielded-palps experiment, and compared this to the change in PN spiking responses to that odour after antennal removal. These two measures were well correlated (Fig. 2d, $n = 20$ odours, Pearson's $r^2 = 0.65$, $P < 0.0001$), which argues that these two experimental paradigms measure the same underlying phenomenon.

The odour tuning of lateral input must reflect the connectivity of the local interneurons that mediate this inhibition. Many individual GABAergic interneurons innervate all glomeruli[9,12,13], suggesting that lateral inhibitory input to each glomerulus might reflect pooled input from all ORNs. If so, then the size of lateral input to a glomerulus should correlate with the total ORN activity evoked by that odour. We estimated total ORN activity by summing the spiking responses of each antennal ORN type[23], and found that this measure predicted the strength of lateral inhibition evoked by each odour in the shielded-palps experiment (Fig. 2e, $n = 14$ odours, Pearson's $r^2 = 0.73$, $P < 0.0005$).

If lateral inhibition to all glomeruli scales with total ORN activity, then lateral inhibitory input to each glomerulus would show the same odour tuning. We have already shown that the odour tuning of lateral input to VM7 is a good predictor of which odour responses were most disinhibited in VM7 PNs after antennal removal (Fig. 2d). As expected, it also partially predicted which odour responses were most disinhibited in a different palp glomerulus, VC1 (Fig. 2f, $n = 20$ odours, Pearson's $r^2 = 0.32$, $P < 0.01$). However, this correlation was weaker than the correlation with disinhibition in VM7. This leaves open the possibility that there may be some differences in the odour tuning of lateral inhibitory input to different glomeruli (see Discussion).

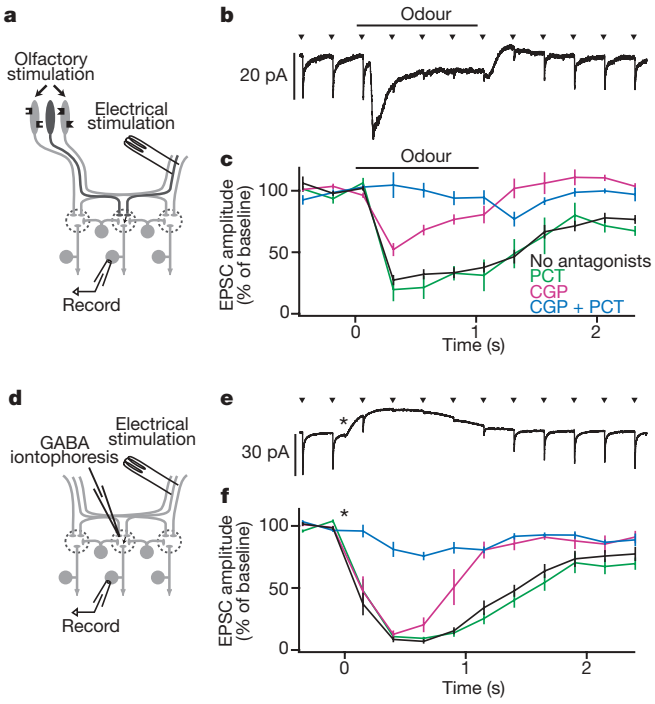

Figure 3 | Lateral GABAergic suppression of ORN–PN synapses. **a**, Experimental configuration. **b**, Electrical stimulation of the antennal nerve (arrowheads) evokes EPSCs in a PN (average of 20 trials). Olfactory stimulation (500 ms) inhibits EPSCs. Odour also evokes a transient inward current reflecting lateral postsynaptic excitation; this is resistant to GABA antagonists (Supplementary Fig. 6). **c**, Inhibition is blocked by the $GABA_B$ antagonist CGP54626 (CGP) together with the $GABA_A$ antagonist picrotoxin (control, $n = 12$; PCT, $n = 5$; CGP, $n = 5$; CGP + PCT, $n = 5$). All pairwise comparisons are significantly different except control versus PCT ($P < 0.05$, t-tests). **d**, Experimental configuration, substituting GABA iontophoresis for olfactory stimulation. **e**, As in **b** for GABA iontophoresis (asterisk). GABA also evokes an outward current. **f**, As in **c** for GABA iontophoresis (control, $n = 13$; PCT, $n = 5$; CGP, $n = 6$; CGP + PCT, $n = 7$). All pairwise comparisons between conditions are significantly different except control versus PCT ($P < 0.05$, t-tests). Data are shown as mean ± s.e.m.

GABA mediates presynaptic inhibition

Our results suggest that much of the lateral inhibition in this circuit acts by suppressing ORN–PN synaptic transmission. To test this, we monitored ORN–PN synaptic strength in one glomerulus while recruiting lateral input to that glomerulus (Fig. 3a). We recorded from an identified PN while electrically stimulating the ipsilateral antennal nerve to evoke excitatory postsynaptic currents (EPSCs). Next, we used an odour to stimulate ORNs in the remaining intact antenna (and the maxillary palps). Because most glomeruli receive bilateral ORN input[2], olfactory stimulation of the contralateral antenna drives activity in ipsilateral glomeruli. Finally, we prevented odours from recruiting direct ORN input to the recorded PN by mutating the odorant receptor gene normally expressed by its ORNs.

As predicted, olfactory stimulation of the contralateral antenna inhibited EPSCs evoked by ipsilateral nerve stimulation (Fig. 3b, c). We could mimic this inhibition by iontophoresing GABA into the antennal lobe neuropil (Fig. 3d–f). A $GABA_B$ receptor antagonist blocked the late phase of this inhibition, but had only a modest effect on the early phase (Fig. 3c, f). Adding a $GABA_A$ antagonist to the $GABA_B$ antagonist blocked the residual early portion of the inhibition (Fig. 3c, f). The $GABA_A$ antagonist alone had no effect (Fig. 3c, f). Taken together, these results suggest that both $GABA_A$ and $GABA_B$ receptors are present on the same ORN axon terminals, and that either $GABA_A$ or $GABA_B$ receptors alone are sufficient to mediate substantial inhibition of EPSCs just after GABA release. The late phase of inhibition evidently involves only $GABA_B$ receptors.

Presynaptic inhibition is generally associated with a change in the way in which a synapse responds to paired electrical pulses[24]. We found that both the $GABA_A$ and the $GABA_B$ components of EPSC inhibition are associated with an increase in the paired-pulse ratio (Supplementary Fig. 7). This implies that the independent actions of both $GABA_A$ and $GABA_B$ receptors are at least partially presynaptic. As a further test of this model, we genetically abolished $GABA_B$ signalling selectively in presynaptic ORNs. We used an ORN-specific promoter[25] to drive expression of pertussis toxin[26]—a selective inhibitor of some types of G proteins. In these flies, GABA still inhibited ORN–PN EPSCs, but now this inhibition had a briefer duration than

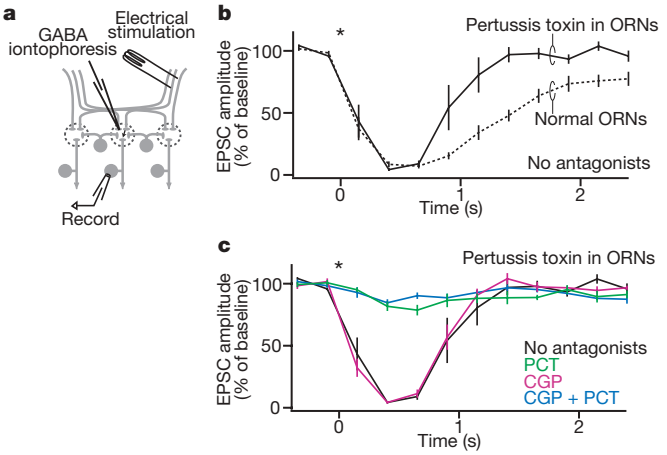

Figure 4 | Genetic evidence that $GABA_B$ receptors inhibit ORN–PN synapses at a presynaptic locus. **a**, Experimental configuration. **b**, When pertussis toxin is specifically expressed in ORNs, GABAergic inhibition of EPSCs (solid line, $n = 11$) is more transient than in control flies (dotted line, $n = 13$, reproduced from Fig. 3f). **c**, Pertussis toxin expression in ORNs renders the GABAergic inhibition of EPSCs completely insensitive to CGP, and completely sensitive to PCT (black trace reproduced from **a**; CGP, $n = 5$; PCT, $n = 6$; CGP + PCT, $n = 5$). Compare to Fig. 3f. Asterisk represents GABA iontophoresis. Data are shown as mean ± s.e.m.

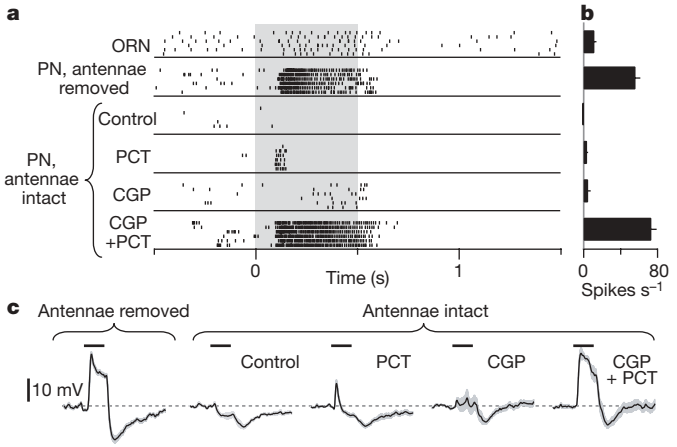

Figure 5 | GABA receptor antagonists mimic removal of lateral input to a projection neuron. **a**, Rasters show spiking responses to pentyl acetate (grey) in a VM7 ORN and a VM7 PN. With antennae intact, both antagonists are required to mimic the effect of antennal removal on PNs. (Some off-inhibition in PNs persists after antennal removal or in the presence of antagonists; this probably reflects the off-inhibition in VM7 ORNs.) **b**, Average spike rates during odour stimulus period, minus baseline spike rates ($n = 5$–6 PNs for each condition). **c**, Average membrane potential responses to pentyl acetate in VM7 PNs ($n = 5$–6 projection neurons for each). Data are shown as mean ± s.e.m.

in wild-type flies (Fig. 4a, b). Unlike in wild-type flies, this inhibition was completely resistant to the $GABA_B$ antagonist and completely blocked by the $GABA_A$ antagonist (compare Fig. 4c to Fig. 3f). As a negative control, we confirmed that this phenotype requires both the ORN-specific promoter and the toxin transgene (Supplementary Fig. 8). This demonstrates that $GABA_B$ receptors inhibit ORN–PN synapses at a purely presynaptic locus.

If activation of either $GABA_A$ or $GABA_B$ receptors is sufficient to mediate strong lateral inhibition, then blockade of both receptors should be required to mimic the removal of lateral input. To test this, we again recorded from palp PNs in glomerulus VM7. Normally, the odour pentyl acetate weakly excites VM7 ORNs and inhibits VM7 PNs. When most lateral input is removed (by removing the antennae), this odour strongly excites these PNs (Fig. 1c). We could not mimic this disinhibition by applying either a $GABA_A$ or a $GABA_B$ receptor antagonist alone. However, the two antagonists together produced strong disinhibition that resembled the effect of removing the antennae (Fig. 5).

Discussion

Many previous studies have shown that odours can inhibit spiking in olfactory bulb mitral cells and antennal lobe PNs (see refs 27–32 for early examples), but in principle this inhibition could be purely intraglomerular[15–17]. Experiments *in vitro* have revealed several types of interglomerular circuits[33–35], but some of these circuits are evidently not recruited by olfactory stimuli[15]. Here we have directly demonstrated an important role for inhibitory interactions between olfactory glomeruli *in vivo*.

Our results argue that a substantial component of interglomerular inhibition occurs at a presynaptic locus. Previous studies in other species have shown that GABA can inhibit release from ORN axon terminals[15–21]. Our results imply that in *Drosophila* this is mediated by both $GABA_A$ and $GABA_B$ receptors. This arrangement is unusual but not unique; for example, there are several instances of $GABA_A$ and $GABA_B$ inhibition at the same presynaptic site in other neural circuits[36–39]. Ionotropic and metabotropic receptors act with different kinetics, and so this arrangement might ensure that inhibition spans a broad time window. Although both receptor types were co-active during most of the odour response, we noticed that $GABA_A$ receptors were required for a brief early phase of inhibition after odour onset (Fig. 5) whereas $GABA_B$ receptors were required for the long, late phase (Figs 3 and 5).

We have shown that lateral inhibitory input to a glomerulus roughly scales with total ORN activity. This would imply that the odour tuning of GABAergic input to each glomerulus is approximately similar. However, the effects of lateral input may nevertheless be somewhat glomerulus-specific. Even if the odour tuning of GABA release were identical in all glomeruli, the efficacy of presynaptic inhibition will vary with presynaptic membrane potential[40,41]. As a result, the same inhibitory signal should be more effective in some glomeruli than in others. Also, in some glomeruli, lateral inhibition might be outweighed by lateral excitation. This would explain why other studies have found that some PNs can be excited by odours that do not excite their cognate ORNs[8,10,12,42].

We propose that this form of gain control represents a flexible balance between sensitivity and efficiency. When total ORN input is weak, lateral inhibition is minimal, and ORN–PN synapses are strong. When an odorant recruits vigorous ORN input to many glomeruli, GABAergic interneurons inhibit ORN neurotransmitter release. This should prevent a stimulus from saturating the dynamic range of many types of PNs simultaneously. Because this mechanism suppresses responses that are strong and redundant, it may tend to decrease cross-correlations between the output of different glomeruli, and thus promote a more efficient neural code for odours.

METHODS SUMMARY

In vivo whole-cell patch-clamp recordings from PNs and extracellular recordings from ORNs were performed essentially as described previously[8–11,42]. Recordings in Fig. 3a–c were made from VM2 PNs in *Or43b*[1] mutant flies. Antagonists (50 μM CGP54626 and 5 μM picrotoxin, PCT) were added to the saline, which perfused the brain. Pertussis toxin was expressed under control of the *Or83b-GAL4* driver. All data are shown as mean values, averaged across experiments, ± s.e.m. (except for raw electrophysiological traces and rasters). The odour stimulus period (shown as a black bar in Figures) was 500 ms, except in Fig. 3b, c.

Full Methods and any associated references are available in the online version of the paper at www.nature.com/nature.

Received 22 September 2007; accepted 25 February 2008.
Published online 16 March 2008.

1. Laissue, P. P. *et al.* Three-dimensional reconstruction of the antennal lobe in *Drosophila melanogaster*. *J. Comp. Neurol.* **405**, 543–552 (1999).

2. Stocker, R. F., Lienhard, M. C., Borst, A. & Fischbach, K. F. Neuronal architecture of the antennal lobe in *Drosophila melanogaster. Cell Tissue Res.* **262,** 9–34 (1990).
3. Couto, A., Alenius, M. & Dickson, B. J. Molecular, anatomical, and functional organization of the *Drosophila* olfactory system. *Curr. Biol.* **15,** 1535–1547 (2005).
4. Fishilevich, E. & Vosshall, L. B. Genetic and functional subdivision of the *Drosophila* antennal lobe. *Curr. Biol.* **15,** 1548–1553 (2005).
5. Marin, E. C., Jefferis, G. S., Komiyama, T., Zhu, H. & Luo, L. Representation of the glomerular olfactory map in the *Drosophila* brain. *Cell* **109,** 243–255 (2002).
6. Wang, J. W., Wong, A. M., Flores, J., Vosshall, L. B. & Axel, R. Two-photon calcium imaging reveals an odor-evoked map of activity in the fly brain. *Cell* **112,** 271–282 (2003).
7. Root, C. M., Semmelhack, J. L., Wong, A. M., Flores, J. & Wang, J. W. Propagation of olfactory information in *Drosophila. Proc. Natl Acad. Sci. USA* **104,** 11826–11831 (2007).
8. Wilson, R. I., Turner, G. C. & Laurent, G. Transformation of olfactory representations in the *Drosophila* antennal lobe. *Science* **303,** 366–370 (2004).
9. Wilson, R. I. & Laurent, G. Role of GABAergic inhibition in shaping odor-evoked spatiotemporal patterns in the *Drosophila* antennal lobe. *J. Neurosci.* **25,** 9069–9079 (2005).
10. Bhandawat, V., Olsen, S. R., Gouwens, N. W., Schlief, M. L. & Wilson, R. I. Sensory processing in the *Drosophila* antennal lobe increases reliability and separability of ensemble odor representations. *Nature Neurosci.* **10,** 1474–1482 (2007).
11. Olsen, S. R., Bhandawat, V. & Wilson, R. I. Excitatory interactions between olfactory processing channels in the *Drosophila* antennal lobe. *Neuron* **54,** 89–103 (2007).
12. Shang, Y., Claridge-Chang, A., Sjulson, L., Pypaert, M. & Miesenbock, G. Excitatory local circuits and their implications for olfactory processing in the fly antennal lobe. *Cell* **128,** 601–612 (2007).
13. Stocker, R. F., Heimbeck, G., Gendre, N. & de Belle, J. S. Neuroblast ablation in *Drosophila* P[GAL4] lines reveals origins of olfactory interneurons. *J. Neurobiol.* **32,** 443–456 (1997).
14. Ng, M. *et al.* Transmission of olfactory information between three populations of neurons in the antennal lobe of the fly. *Neuron* **36,** 463–474 (2002).
15. McGann, J. P. *et al.* Odorant representations are modulated by intra- but not interglomerular presynaptic inhibition of olfactory sensory neurons. *Neuron* **48,** 1039–1053 (2005).
16. Murphy, G. J., Darcy, D. P. & Isaacson, J. S. Intraglomerular inhibition: signaling mechanisms of an olfactory microcircuit. *Nature Neurosci.* **8,** 354–364 (2005).
17. Vucinic, D., Cohen, L. B. & Kosmidis, E. K. Interglomerular center-surround inhibition shapes odorant-evoked input to the mouse olfactory bulb *in vivo. J. Neurophysiol.* **95,** 1881–1887 (2006).
18. Nickell, W. T., Behbehani, M. M. & Shipley, M. T. Evidence for $GABA_B$-mediated inhibition of transmission from the olfactory nerve to mitral cells in the rat olfactory bulb. *Brain Res. Bull.* **35,** 119–123 (1994).
19. Wachowiak, M. & Cohen, L. B. Presynaptic inhibition of primary olfactory afferents mediated by different mechanisms in lobster and turtle. *J. Neurosci.* **19,** 8808–8817 (1999).
20. Aroniadou-Anderjaska, V., Zhou, F. M., Priest, C. A., Ennis, M. & Shipley, M. T. Tonic and synaptically evoked presynaptic inhibition of sensory input to the rat olfactory bulb via $GABA_B$ heteroreceptors. *J. Neurophysiol.* **84,** 1194–1203 (2000).
21. Wachowiak, M. *et al.* Inhibition of olfactory receptor neuron input to olfactory bulb glomeruli mediated by suppression of presynaptic calcium influx. *J. Neurophysiol.* **94,** 2700–2712 (2005).
22. Distler, P. G. & Boeckh, J. Synaptic connections between identified neuron types in the antennal lobe glomeruli of the cockroach, Periplaneta americana: II. Local multiglomerular interneurons. *J. Comp. Neurol.* **383,** 529–540 (1997).
23. Hallem, E. A. & Carlson, J. R. Coding of odors by a receptor repertoire. *Cell* **125,** 143–160 (2006).
24. Zucker, R. S. & Regehr, W. G. Short-term synaptic plasticity. *Annu. Rev. Physiol.* **64,** 355–405 (2002).
25. Larsson, M. C. *et al. Or83b* encodes a broadly expressed odorant receptor essential for *Drosophila* olfaction. *Neuron* **43,** 703–714 (2004).
26. Ferris, J., Ge, H., Liu, L. & Roman, G. G(o) signaling is required for *Drosophila* associative learning. *Nature Neurosci.* **9,** 1036–1040 (2006).
27. Shibuya, T., Ai, N. & Takagi, S. F. Response types of single cells in the olfactory bulb. *Proc. Jpn. Acad.* **38,** 231–233 (1962).
28. Macrides, F. & Chorover, S. L. Olfactory bulb units: activity correlated with inhalation cycles and odor quality. *Science* **175,** 84–87 (1972).
29. Mathews, D. F. Response patterns of single units in the olfactory bulb of the rat to odor. *Brain Res.* **47,** 389–400 (1972).
30. Tanabe, T., Iino, M. & Takagi, S. F. Discrimination of odors in olfactory bulb, pyriform-amygdaloid areas, and orbitofrontal cortex of the monkey. *J. Neurophysiol.* **38,** 1284–1296 (1975).
31. Meredith, M. & Moulton, D. G. Patterned response to odor in single neurones of goldfish olfactory bulb: influence of odor quality and other stimulus parameters. *J. Gen. Physiol.* **71,** 615–643 (1978).
32. Chaput, M. & Holley, A. Single unit responses of olfactory bulb neurones to odour presentation in awake rabbits. *J. Physiol. (Paris)* **76,** 551–558 (1980).
33. Isaacson, J. S. & Strowbridge, B. W. Olfactory reciprocal synapses: dendritic signaling in the CNS. *Neuron* **20,** 749–761 (1998).
34. Urban, N. N. & Sakmann, B. Reciprocal intraglomerular excitation and intra- and interglomerular lateral inhibition between mouse olfactory bulb mitral cells. *J. Physiol. (Lond.)* **542,** 355–367 (2002).
35. Aungst, J. L. *et al.* Centre-surround inhibition among olfactory bulb glomeruli. *Nature* **426,** 623–629 (2003).
36. Stuart, G. J. & Redman, S. J. The role of $GABA_A$ and $GABA_B$ receptors in presynaptic inhibition of Ia EPSPs in cat spinal motoneurones. *J. Physiol. (Lond.)* **447,** 675–692 (1992).
37. Matthews, G., Ayoub, G. S. & Heidelberger, R. Presynaptic inhibition by GABA is mediated via two distinct GABA receptors with novel pharmacology. *J. Neurosci.* **14,** 1079–1090 (1994).
38. Fischer, Y. & Parnas, I. Differential activation of two distinct mechanisms for presynaptic inhibition by a single inhibitory axon. *J. Neurophysiol.* **76,** 3807–3816 (1996).
39. Fischer, Y. & Parnas, I. Activation of $GABA_B$ receptors at individual release boutons of the crayfish opener neuromuscular junction produces presynaptic inhibition. *J. Neurophysiol.* **75,** 1377–1385 (1996).
40. Bean, B. P. Neurotransmitter inhibition of neuronal calcium currents by changes in channel voltage dependence. *Nature* **340,** 153–156 (1989).
41. Foldy, C., Neu, A., Jones, M. V. & Soltesz, I. Presynaptic, activity-dependent modulation of cannabinoid type 1 receptor-mediated inhibition of GABA release. *J. Neurosci.* **26,** 1465–1469 (2006).
42. Schlief, M. L. & Wilson, R. I. Olfactory processing and behavior downstream from highly selective receptor neurons. *Nature Neurosci.* **10,** 623–630 (2007).

Supplementary Information is linked to the online version of the paper at www.nature.com/nature.

Acknowledgements We thank K. Ito, L. Luo, G. Roman, D. P. Smith, L. M. Stevens and L. B. Vosshall for gifts of fly stocks. We thank G. Laurent, A. W. Liu and members of the Wilson laboratory for conversations. This work was funded by a grant from the NIDCD, the Pew, McKnight, Sloan, and Beckman Foundations (to R.I.W.). S.R.O. was partially supported by a NSF fellowship.

Author Contributions S.R.O. performed the experiments and analysed the data. S.R.O. and R.I.W. designed the experiments and wrote the paper.

Author Information Reprints and permissions information is available at www.nature.com/reprints. Correspondence and requests for materials should be addressed to R.I.W. (rachel_wilson@hms.harvard.edu).

METHODS

Fly stocks. Flies were reared at 20–21 °C on conventional cornmeal agar. All experiments were performed on adult female flies 2–5 days post-eclosion. Fly stocks were provided as follows: *Or43b*[1] (D. Smith); *NP5103-GAL4*, *NP3481-GAL4* and *NP5221-GAL4* (K. Ito and L. Luo); *Or46a-GAL4* and *Or83b-GAL4* (L. Vosshall); *UAS-DTl*$_{II}$ and *UAS-DTl*$_{III}$ (L. Stevens); *UAS-PTX* (G. Roman); and *UAS-CD8GFP*$_{I}$ (Bloomington Stock Center).

ORN recordings. Extracellular recordings of ORN spiking were performed as described previously[10]. To accurately sort spikes recorded from VC1 ORNs, we killed the second ORN type (VA7l) housed in the same sensillum. This was done by expressing diphtheria toxin light chain in the VA7l ORNs (genotype: either *Or46a-GAL4/UAS-DTl*$_{II}$ ($n = 4$) or *Or46a-GAL4/+; UAS-DTl*$_{III}$*/+* ($n = 4$)). The genotype for VM7 ORN recordings was *NP3481-Gal4 UAS-CD8GFP*, which is the same genotype as that used for the VM7 PN recordings. VM7 ORNs fire spontaneously at 10 spikes s^{-1}, and VC1 ORNs fire spontaneously at 3 spikes s^{-1}.

Projection neuron recordings. *In vivo* whole-cell recordings from PNs were performed as previously described[10]. For the current-clamp recordings in Figs 1, 2 and 5 and in Supplementary Figs 2–5, the composition of the internal patch-pipette solution was (in mM): potassium aspartate 140, HEPES 10, MgATP 4, Na_3GTP 0.5, EGTA 1, KCl 1, and biocytin hydrazide 13 (pH 7.3, osmolarity adjusted to ~265 mOsm). For the voltage-clamp recordings in Figs 3 and 4 and Supplementary Figs 6–8, the composition of the internal was (in mM): cesium aspartate 140, HEPES 10, MgATP 4, Na_3GTP 0.5, EGTA 1, KCl 1, biocytin hydrazide 13, and QX-314 10 (pH 7.3, osmolarity adjusted to ~265 mOsm). The composition of the external saline solution in all recordings was (in mM): NaCl 103, KCl 3, *N*-tris(hydroxymethyl) methyl-2-aminoethanesulfonic acid 5, trehalose 8, glucose 10, $NaHCO_3$ 26, NaH_2PO_4 1, $CaCl_2$ 1.5, and $MgCl_2$ 4. Osmolarity was adjusted to 270–275 mOsm. The saline was bubbled with 95% O_2/5% CO_2 and reached a final pH of 7.3. Saline perfused the brain continuously at 2 ml min^{-1}. Recordings were obtained with an A-M Systems Model 2400 amplifier (100 MΩ headstage), were low-pass filtered at 5 kHz, and digitized at 10 kHz. Data were acquired in Igor Pro. In most experiments, we used an enhancer trap line to label specific PNs with green fluorescent protein (GFP) for targeted recording. VM7 PNs were labelled by *NP3481-Gal4 UAS-CD8GFP* (Figs 1, 2 and 5, and Supplementary Figs 2, 4 and 5). VC1 PNs were labelled by *NP5221-Gal4 UAS-CD8GFP* (Fig. 1 and Supplementary Fig. 3). VM2 PNs were labelled by *NP5103-Gal4 UAS-CD8GFP* (Fig. 3a–c, and Supplementary Fig. 6a–c and the 'odour' condition in Supplementary Fig. 7d). VM2 PNs were recorded in flies in which the odorant receptor expressed by VM2 ORNs was mutated (*NP5103-Gal4 UAS-CD8GFP; Or43b*[1], see schematic in Fig. 3a). In some experiments for each genotype, we filled the recorded cell with biocytin and verified the PN identity with biocytin histochemistry as described previously[8]. In the GABA iontophoresis experiments in Fig. 3d–f (also Supplementary Figs 6d–f and 7), we recorded from PNs in the anterodorsal cell cluster[5] labelled by the enhancer trap line *GH146* (*GH146-Gal4 UAS-CD8GFP*). For the experiments in which pertussis toxin was selectively expressed in ORNs (Fig. 4, also Supplementary Fig. 8), we recorded from PNs in the anterodorsal cell cluster in the genotype *Or83b-Gal4; UAS-PTX/+*. In voltage-clamp recordings, the command potential was either −85 mV (Fig. 3a–c) or −65 mV (Figs 3d–f and 4).

Manipulation of peripheral organs. Antennal input was abolished in some experiments by severing the antennal nerves with fine forceps just before recording. The antennal nerve was gently broken by applying forces perpendicular to the long axis of the nerve, leaving a stump of nerve attached to the antennal lobe. In other experiments, the maxillary palps were removed with forceps just before recording. For both antennal and palp amputation, the cell bodies of the affected ORNs are removed, but the proximal portions of their axons remain intact and continue to innervate the antennal lobe. Amputation removes ORN somata and thus large spontaneous spike-driven EPSCs (~5–20 pA) disappear almost entirely. Axon terminals are still intact, as evidenced by the persistence of miniature EPSCs (~1 pA). In some experiments, the maxillary palps were shielded from direct odour stimulation by covering them in '5 minute epoxy' (Devcon). The epoxy was allowed to dry for ~20 min before the recording was started. We confirmed that this substance is relatively non-toxic to ORNs by covering the antennae in epoxy, allowing it to dry, peeling the epoxy away, and verifying that odours were still able to elicit a normal field-potential response in the antennae.

Olfactory stimulation. Odours were diluted in paraffin oil at a ratio of 1:100 v/v. Odour dilutions in paraffin oil were prepared fresh every 5 days. Our odour panel consisted of benzaldehyde, butyric acid, 1-butanol, cyclohexanone, ethyl butyrate, ethyl acetate, ethyl-3-hydroxybutryate, fenchone, geranyl acetate, 2-heptanone, linalool, 4-methyl cyclohexanol, methyl salicylate, 3-methylthio-1-propanol, 4-methyl phenol, octanal, 1-octen-3-ol, pentyl acetate, trans-2-hexenal and paraffin oil (solvent control). Odour source details are posted at http://wilson.med.harvard.edu/odors.html. Odours were delivered with a custom-built olfactometer as described previously[10]. Odour stimuli were applied for 500 ms, except in Fig. 3 in which the odour was applied for 1 s. For the experiments in Figs 1, 2 and 5, consecutive odour presentations were spaced 25–35 s apart.

Direct ORN axon stimulation. In Figs 3 and 4 and in Supplementary Figs 6–8, we electrically stimulated ORN axons. The ipsilateral antennal nerve was severed and inserted into a stimulating suction electrode. Single spikes were evoked in ORN axons with a short current pulse (50 μs) using a stimulus isolator (A.M.P.I.). In each sweep we delivered a train of 23 nerve stimuli at 4 Hz. During the train, the size of the evoked EPSCs decreased over the first 4–8 stimuli owing to short-term depression, but then reached a steady value. We timed our GABA iontophoresis and odour stimulation to occur during this steady-state period. For the paired-pulse experiments in Supplementary Fig. 7, we delivered two electrical stimuli to the nerve with an inter-pulse interval of 25 ms. This interval produces depression at the ORN–PN synapse under control conditions and allowed us to observe increases in the paired-pulse ratio when we decreased release probability.

GABA iontophoresis. In the GABA iontophoresis experiments, a high-resistance (~80 ΩM) sharp glass pipette was filled with a solution of 250 mM GABA in water, and the pH was adjusted to 4.3 by adding HCl. GABA was ejected into the antennal lobe neuropil with a brief (3–20 ms) positive current pulse using an iontophoresis unit (World Precision Instruments). A constant negative backing current was applied to retain GABA in the iontophoresis pipette between ejection events. To ensure that a similar amount of GABA was released into the neuropil in all experiments, and that the time-course of GABA release was as consistent as possible, we adjusted the location of the iontophoresis pipette, the level of negative backing current and the duration of the ejection current at the beginning of each experiment. We did not proceed with an experiment until the following criteria were met: EPSC suppression was ~50% at 150 ms after iontophoresis, maximal EPSC suppression was ~85% at 400 ms after iontophoresis, and GABA evoked an outward current in the recorded PN which lasted for ~1–1.5 s.

Antagonists. Antagonists were prepared as concentrated stock solutions and a measured volume of stock was added to the saline perfusate to achieve the final drug concentrations. Picrotoxin (Sigma) was used at 5 μM, CGP54626 (Tocris) was used at 50 μM, and $CdCl_2$ (Sigma) was used at 10–25 μM.

Peri-stimulus time histograms. For the experiments in Figs 1 and 5 and in Supplementary Figs 2 and 3, spike times were extracted from raw ORN and PN recordings using routines in Igor Pro. Each cell was tested with multiple odours, and each odour was presented six times. The response to the first presentation was not included in our analysis. Each of the five remaining trials was converted into a peri-stimulus time histogram (PSTH) by counting the number of spikes in 50-ms bins that overlapped by 25 ms. These single-trial PSTHs were averaged together to generate a PSTH describing the response to an odour in a given experiment. Multiple cells corresponding to each glomerular class and each cell type (ORN or PN) were tested with a given odour in multiple experiments. Average PSTHs in Fig. 1 and Supplementary Figs 2 and 3 represent the mean ± s.e.m. computed across experiments.

Input–output functions. For the analysis of odour responses in Fig. 1d, we computed the average spike rate over the 500-ms odour duration and subtracted the baseline firing rate averaged over the 500-ms window before odour onset. Each point in the input–output function represents the mean PN response to an odour plotted against the mean response of the cognate ORNs to the same odour. Fits are single exponential functions.

Lifetime sparseness. The selectivity of a neuron's odour response profile (Fig. 1e) was quantified as lifetime sparseness:

$$S = \frac{1}{1-1/N}\left(1 - \frac{\left(\sum_{j=1}^{N} r_j/N\right)^2}{\sum_{j=1}^{N} r_j^2/N}\right)$$

where N = the number of odours and r_j is the analogue response intensity of the neuron to odour j minus baseline firing rate. Analogue response intensity was the mean spike rate (averaged across five sweeps) during the entire 500-ms odour stimulus period. Any values of $r_j < 0$ were set to zero before computing lifetime sparseness (this was the only analysis in this study in which negative responses were zeroed). Responses to paraffin oil (solvent control) were not considered in the sparseness analysis. We computed the lifetime sparseness for each individual cell in our study for which we tested at least 12 of the odours in our set. We used the Mann–Whitney *U*-test to assess the significance of sparseness differences.

Correlations between ranked odour preferences. To compute correlations between ORN and PN odour preferences, we computed Spearman's rank correlation coefficient (ρ) on the odour response vectors of these neurons. This is a

nonparametric measure that quantifies how well any monotonic function could describe the relationship between ORN and PN responses. We chose this rather than a linear (Pearson's) correlation coefficient because the intrinsic input–output function of these glomeruli is highly nonlinear (Fig. 1d). For each glomerulus, we computed Spearman's ρ on each pairwise combination of individually recorded ORNs and PNs for which we tested at least 12 of the same odours on both cells (for glomerulus VM7, $n = 27$ comparisons for ORNs compared to PNs with antennae and $n = 38$ for ORNs compared to PNs without antennae; for glomerulus VC1, $n = 19$ for ORNs compared to PNs with antennae and $n = 25$ for ORNs compared to PNs without antennae). We report the mean of these pairwise correlations. We assessed the significance of differences in Spearman's ρ with the Mann–Whitney *U*-test.

Quantifying changes in membrane potential. In Figs 2c and 5c, we show membrane potential responses averaged across multiple experiments. To generate these we first averaged 4–6 consecutive sweeps within a single experiment for each odour and low-pass filtered this at 13 Hz to remove any spikes. Next we averaged these responses across experiments, with ± s.e.m. shown in pastel. To quantify the magnitude of lateral input in Fig. 2d–f, we integrated the change in membrane potential (versus baseline) over a 2-s interval beginning at odour onset. We chose this interval because shorter intervals did not capture as much odour dependence in the magnitude of lateral input. In Fig. 2d, f, PN disinhibition was computed by averaging PN firing rates over the 2 s after odour onset, and then averaging across experiments (4–12 PNs per odour), before computing the difference in the PN responses with antennae versus without antennae. In Fig. 2e, total ORN activity for each odour was computed by summing all the response rates in ref. 23. There are only 14 data points in this panel because only 14 of our odours were included in ref. 23.

EPSC amplitudes. We measured EPSC amplitudes in Figs 3 and 4 and in Supplementary Figs 6–8 by first averaging together a block of 8–20 sweeps from the same experiment. From these averaged traces, we computed the EPSC amplitude as the average over a 0.9-ms window centred on the peak. Before averaging across experiments, we normalized the train of evoked EPSCs to the baseline EPSCs evoked just before either odour or GABA onset.